Separation and Identification of Structural Isomers by Quadrupole Collision-Induced Dissociation-Hydrogen/Deuterium Exchange-Infrared Multiphoton Dissociation (QCID-HDX-IRMPD)

Ashley C. Gucinski,[a] Árpád Somogyi,[a] Julia Chamot-Rooke,[b] and Vicki H. Wysocki[a]

[a] Department of Chemistry and Biochemistry, University of Arizona, Tucson, Arizona, USA
[b] Laboratoire des Mecanismes Reactionnels, Department of Chemistry, Ecole Polytechnique and CNRS, Palaiseau, France

A new approach that uses a hybrid Q-FTICR instrument and combines quadrupole collision-induced dissociation, hydrogen-deuterium exchange, and infrared multiphoton dissociation (QCID-HDX-IRMPD) has been shown to effectively separate and differentiate isomeric fragment ion structures present at the same *m/z*. This method was used to study protonated YAGFL-OH (free acid), YAGFL-NH_2 (amide), cyclic YAGFL, and YAGFL-OCH_3 (methyl ester). QCID-HDX of *m/z* 552.28 ($C_{29}H_{38}N_5O_6$) from YAGFL-OH reveals at least two distributions of ions corresponding to the b_5 ion and a non-C-terminal water loss ion structure. Subsequent IRMPD fragmentation of each population shows distinct fragmentation patterns, reflecting the different structures from which they arise. This contrasts with data for YAGFL-NH_2 and YAGFL-OCH_3, which do not show two distinct H/D exchange populations for the $C_{29}H_{38}N_5O_6$ structure formed by NH_3 and $HOCH_3$ loss, respectively. Relative extents of exchange for $C_{29}H_{38}N_5O_6$ ions from six sequence isomers (YAGFL, AGFLY, GFLYA, FLYAG, LYAGF, and LFGAY) show a sequence dependence of relative isomer abundance. Supporting action IRMPD spectroscopy data are also presented herein and also show that multiple structures are present for the $C_{29}H_{38}N_5O_6$ species from YAGFL-OH. (J Am Soc Mass Spectrom 2010, 21, 1329–1338) © 2010 Published by Elsevier Inc. on behalf of American Society for Mass Spectrometry

Tandem mass spectrometry is widely used for the identification of peptides and proteins [1, 2]. Generally, protonated peptides at a given *m/z* are selected and fragmented via collision-induced dissociation (CID), generating 'b' and 'y' fragment ions, which allows the peptide sequence to be determined.

In the course of a common proteomics experiment, several hundred to several thousand spectra are generated for a single sample, making manual interpretation of the peptide fragmentation spectra impractical. To speed up the assignment of MS/MS spectra, protein identification algorithms are often used [3, 4]. These algorithms generate theoretical peptide spectra or *m/z* lists based loosely on prevalent fragmentation models, including the mobile proton model [5] and the pathways-in-competition model [6], and compare them with experimental spectra to determine peptide sequences. While these models can help to predict many trends in peptide fragmentation, actual dissociation chemistry is much more complex, and the complete dissociation chemistry in an MS/MS spectrum cannot always be accurately predicted by using existing theoretical models. As a result, false and missed identifications frequently occur, with only a small percentage of the spectra being correctly assigned [7–10]. Incorporation of additional chemical information and fragmentation models into sequencing algorithms could depict fragmentation processes more completely, potentially allowing more accurate kinetic modeling of spectra to be possible, and the success of identification algorithms would likely improve.

One potential cause for missed or false identifications of peptide fragmentation spectra is the presence of multiple isomeric ion structures at a single *m/z*. If multiple isomers are present at one *m/z*, the MS/MS spectrum of that *m/z* could contain fragments from each of the structures present. For example, the b_n ions from peptides of length *n* and the corresponding $[MH - H_2O]^+$ ions are isomeric. While water loss at the peptide C-terminus results in b_5 ion formation for pentapeptides, water can also be lost involving oxygen from an

Address reprint requests to Dr. V. H. Wysocki, Department of Chemistry and Biochemistry, University of Arizona, 1306 E. University Blvd., Tucson, AZ 85721, USA. E-mail: vwysocki@email.arizona.edu

1044-0305/10/$32.00
doi:10.1016/j.jasms.2010.03.036

Published online April 2, 2010
Received December 21, 2009
Revised March 8, 2010
Accepted March 10, 2010

internal carbonyl. This results in a different ion structure that is isomeric with the b_5 ion, referred to as a non-C-terminal water loss ion. Evidence for the formation of non-C-terminal $[MH - H_2O]^+$ ions has been previously reported by Ballard and Gaskell as well as O'Hair and coworkers; a retro-Ritter-type mechanism was proposed for the formation of these product ion structures [11–13]. However, these ions are not routinely incorporated into sequencing algorithms, even for multistep fragmentation pathways, despite the fact that the formation of non-C-terminal $[MH - H_2O]^+$ ions has been shown previously. The presence of multiple uncharacterized fragment ion isomers could significantly complicate the kinetic modeling of the fragmentation process, making the accurate prediction of fragment ion abundances more problematic. Separation of the $[MH - H_2O]^+$ structure from the b_5 structure in spectral interpretation could therefore lead to improved kinetic modeling of peptide fragmentation because it would enable the structures to be modeled separately or, alternatively, corrections could be made to account for multiple structures.

Here we present a new approach that combines quadrupole CID, hydrogen-deuterium exchange, and infrared multiphoton dissociation (QCID-HDX-IRMPD) in an FTICR mass spectrometer for the separation and characterization of isomeric ions in the gas-phase. While this study focuses on an example of isomeric peptide fragment ions generated from the pentapeptide YAGFL-OH and its analogues, this technique can be applied to other isobaric ion species. In the QCID-HDX-IRMPD approach, fragment ions are generated after selection of the precursor ions by the quadrupole and subsequent fragmentation by low-energy (eV) CID in the collision cell. To determine if multiple ion structures are present, all ions (including all fragment and precursor ions) are subjected to HDX in the ICR cell. Because differences in gas-phase structure will allow for different extents and relative rates of HDX, [14] *m/z* values consisting of multiple isomeric ion structures can be identified by the presence of multiple HDX populations for a given product ion *m/z*. The use of HDX to separate isomers has been previously demonstrated by other researchers, including Marshall and coworkers [15] for a series of bradykinins, Herrmann et al. [16] for bradykinin and angiotensin analogues in combination with SORI, Lifshitz and coworkers [17] for isomers of serine octamers, and very recently by Polfer and coworkers for fragments of poly-glycine peptides [18] as well by Somogyi and Paizs to reveal b_2 ion structures [19]. For additional confirmation of the presence of different structures, IRMPD can be used to fragment ions that have been separated by differences in HDX rates. Ultimately, differences in the IRMPD fragmentation patterns can be related to differences in ion structure. This approach is of great utility because it allows for separation and characterization of isomeric ions in the gas phase using a single instrument and experiment per precursor ion. The method proposed herein provides more information than the previously described SORI-HDX method also for an FTICR instrument because of the additional stage of IRMPD fragmentation that provides subsequent MS^3 information on ions with different extents of exchange [20].

The integration of QCID-HDX-IRMPD as a tool for the gas-phase study of ions will complement existing techniques. After many years of characterization by MS/MS, the study of isomeric gas-phase ion structures has been recently the domain of ion mobility-mass spectrometry (IM-MS) and action IRMPD spectroscopy. Gaskell and coworkers used IM-MS to identify both oxazolone and macrocyclic structures for the b_5 ion from YAGFL-NH_2, while Clemmer and coworkers used a similar approach to identify linear and macrocyclic structures for the a_4 and b_4 fragment ions from leucine enkephalin [21, 22]. Variable wavelength action IRMPD spectroscopy has been recently employed by several research groups for the study of gas-phase ions [23–26] and has also been the subject of two recent, extensive reviews [27, 28]. Action IRMPD spectroscopy is ideal for structural characterization of ions, as the IR spectra generated depict the vibrational modes of selected ions, which can be directly correlated to structural features. Polfer and coworkers used this technique to probe the b_4 ion structure of leucine enkephalin (YGGFL), which they discerned to have both macrocyclic and oxazolone structures [29].

The QCID-HDX-IRMPD approach will be illustrated here for YAGFL-OH. This approach clearly shows that fragmentation of YAGFL-OH produces two isomers of $C_{29}H_{38}N_5O_6$ (*m/z* 552.28), the b_5 ion and the non-C-terminal water loss ion. Separation of the isomers is first achieved as a result of the differing HDX kinetics for the b_5 versus non-C-terminal water loss ion structures. The influence of sequence on relative HDX kinetics is also illustrated for six different precursor analogues of the *m/z* 552.28 ion (YAGFL, AGFLY, GFLYA, FLYAG, LYAGF, and LFGAY). The combined QCID-HDX-IRMPD technique results in the generation of fragmentation spectra of ions from different HDX populations which reflect the differences in structure of the b_5 and non-C-terminal water loss ions. These results are correlated with action IRMPD dissociation spectra. The work presented here suggests that QCID-HDX-IRMPD could potentially serve as a pre-screening tool to determine if multiple isomeric structures are reflected in an MS/MS spectrum before variable wavelength action IRMPD spectroscopy is performed.

Experimental

YAGFL-OH and YAGFL sequence analogues were synthesized in house using standard Wang resin solid-phase peptide synthesis [30]. Wang resins and Fmoc-protected residues were obtained from Novabiochem (San Diego, CA, USA). YAGFL-NH_2 was obtained from American Peptide Company (Sunnyvale, CA, USA). Cyclic YAGFL was obtained from Celtek Peptide Com-

pany (Nashville, TN, USA). CD_3OD (99.9%) for use in HDX was purchased from Cambridge Isotope Laboratories (Andover, MA, USA). All other reagents and solvents were purchased from Sigma Aldrich (St. Louis, MO, USA) and used without further purification. To obtain the C-terminal YAGFL methyl ester (YAGFL-OCH_3), ~100 μg of solid peptide was combined in anhydrous methanol with 30 μL 1M acetyl chloride and allowed to react for at least 2 h.

Peptide solutions (ca. 1 μM) were diluted with electrospray solvent (1:1:0.1% water:acetonitrile:formic acid) and introduced into the mass spectrometer via electrospray ionization (ESI) using an Apollo II ESI source and a mechanical syringe pump at a flow rate of 160 μL/h. The precursor ion was monoisotopically selected by the quadrupole (Q) of a Bruker 9.4 T Apex Qh tandem FT-ICR instrument (Bruker Daltonics, Billerica, MA, USA), and collided with Ar at low laboratory collision energies (8–12 eV) in the collision cell (QCID). All fragment ions and the unfragmented precursor ions were then simultaneously transferred to the ICR cell and allowed to undergo HDX reactions for different amounts of time. The present implementation applies a variable number of short valve pulses (50 ms pulses) of CD_3OD reagent into the ICR cell. These pulses are normally separated by 1s and during this time, the pressure in the ICR cell does not drop in a measurable manner. The CD_3OD pressure in the cell was not constant, but the individual pulses are reproducible so that the ability to study relative HDX kinetics is not compromised (i.e., the experimental conditions can be considered the same for all fragment ions and the precursor ion because all enter the cell and are stored simultaneously). After a variable number of pulses the residual CD_3OD is pumped away for a variable period of time (30 s was used for the experiments described here). Following HDX, fragment ions (such as the b_5 ion) can be selected by *m/z* so that ions with different degrees of exchange (D_n) can be isolated within the ICR cell and then activated by IRMPD. IRMPD was used as the final dissociation method instead of SORI because of software limitations, but SORI can also be an applicable final activation step. Standard Bruker IRMPD equipment was used for these experiments (continuous CO_2 laser with a 10.6 μm wavelength and maximum power of 25 W). The laser power and pulse length were controlled by the computer via data acquisition parameters. Typical laser powers and pulse lengths were in the range of 50% to 55% of the maximum power and 0.7 to 1.0 s. For comparisons of different structures, the QCID collision energy, the HDX pulse sequences, the time the ions were allowed to undergo H/D exchange and IRMPD parameters were held constant throughout the experiment to ensure that differences in the fragmentation spectra arise solely from ion structural differences. The typical CD_3OD pressure measured external to the inlet valve was ~15 mbar. The ICR cell base pressure was about 1×10^{-9} Torr, fluctuating between 10^{-7} and 10^{-8} Torr during HDX experiments. Bruker Daltonics DataAnalysis software (ver. 3.4) was used for data analysis.

IRMPD action spectra were acquired at the CLIO Free Electron Laser Facility (Orsay, France) as described previously [26]. Briefly, peptides were fragmented in a modified Bruker Esquire 3000+ ion trap mass spectrometer by using CID. The fragments at *m/z* 552.28 were isolated and fragmented by the CLIO variable wavelength laser. Laser power varied from ~0.5 to 1 W across the spectrum and the spectra are not power-corrected. As the wavelength of the laser was varied from ~1100 to 2050 cm^{-1}, fragmentation of the *m/z* 552.28 ion was achieved when the vibrational frequency of the bonds in the ion match the applied frequency, resulting in the production of the action IRMPD spectrum. The sum of the intensity of the fragment ions relative to the intensity of the *m*/z 552.28 (*m/z* 594.30 for Ac-YAGFL) precursor at each wavelength was used to construct the experimental spectrum by using an in house perl script program.

Results and Discussion

QCID-IRMPD

The *m/z* 552.28 ($C_{29}H_{38}N_5O_6$) generated from QCID of protonated YAGFL-OH and YAGFL-NH_2 and from protonation of cyclic YAGFL were selected in the ICR cell and fragmented by IRMPD. The corresponding MS^3 fragmentation spectra of $C_{29}H_{38}N_5O_6$ (MS^2 for cyclic YAGFL) are shown in Figure 1. While naturally occurring peptides are predominantly found with a C-terminal free acid, recent studies involving the YAGFL system have used the amidated peptide analogues, so YAGFL-NH_2 was included for comparison [31, 32]. YAGFL-NH_2 must lose NH_3 to form the b_5 species, while the free acid forms the b_5 ion through H_2O loss. For the YAGFL-NH_2 the water loss and b_5 ion (ammonia loss) structures are not isobaric, but for YAGFL-OH, the b_5 and non-C-terminal water loss ions have identical molecular formulae. In addition to the overlap of the b_5 and non-C-terminal water loss ions from YAGFL-OH, recent studies have shown that the b_5 ions from YAGFL can have both an oxazolone and macrocyclic structure [31, 32]. The IRMPD MS/MS spectrum of protonated cyclic YAGFL is therefore included in Figure 1 to show how an initially macrocyclic YAGFL b_5 ion would fragment, in comparison with the fragmentation spectrum of $[YAGFL\text{-}NH_3]^+$, which would have a b_5 population with both oxazolone and macrocyclic structures.

Many of the same fragment ions are present in the *m/z* 552.28 ($C_{29}H_{38}N_5O_6$) IRMPD MS^3 fragmentation spectra from YAGFL-OH and YAGFL-NH_2 and the MS/MS spectrum of cyclic YAGFL shown in Figure 1. Predominant fragments include b_5-H_2O (*m/z* 534.28), b_5-CO-NH_3 (*m/z* 507.26), and b_4-NH_3-CO (*m/z* 394.17). However, a characteristic fragment in Figure 1a is the fragment at *m/z* 417.21, corresponding to the loss of the neutral analogue of the tyrosine immonium ion (exact

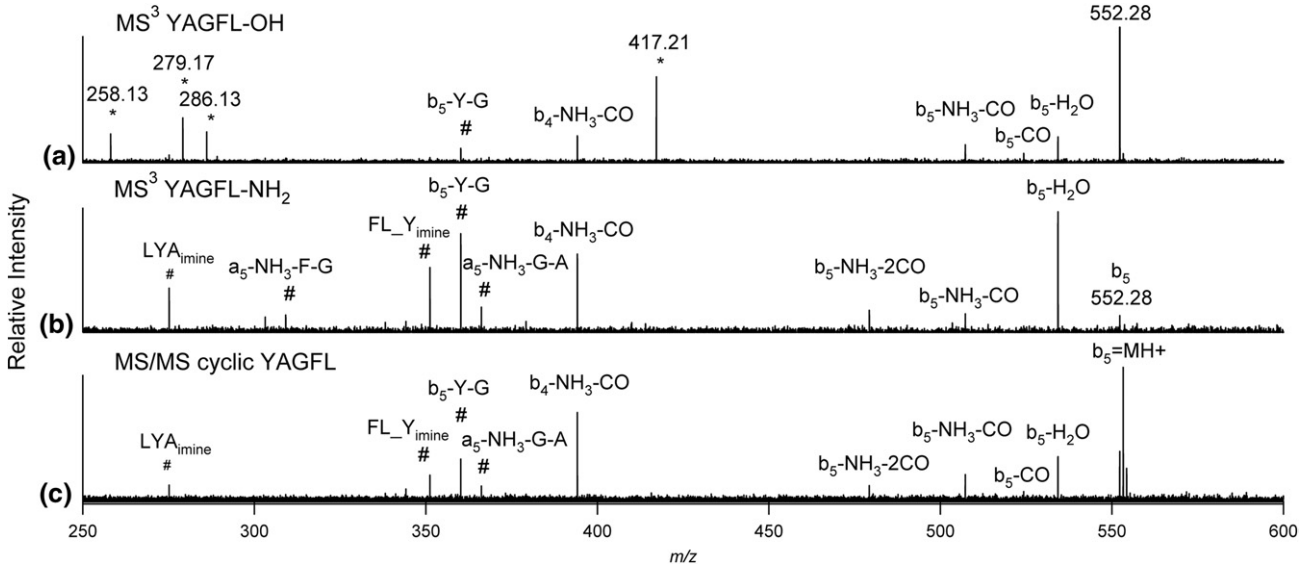

Figure 1. IRMPD MS^3 spectra of ions at *m/z* 552.28 ($C_{29}H_{38}N_5O_6$) generated from QCID (10 eV) from protonated (**a**) YAGFL-OH, (**b**) YAGFL-NH_2, and (**c**) MS/MS of the MH^+ of cyclic YAGFL. (#) Indicates sequence scrambled ions and (*) denotes ions from the non-C-terminal water loss ion structure.

mass 417.2132, elemental composition $C_{21}H_{29}N_4O_5$). If the b_5 ion structure is assumed to be either an oxazolone or a macrocyclic pentapeptide, such a loss of tyrosine would indicate either a neutral loss of the N-terminal amino acid residue or the favored loss of tyrosine as one of five residues. Neither of these is a common peptide

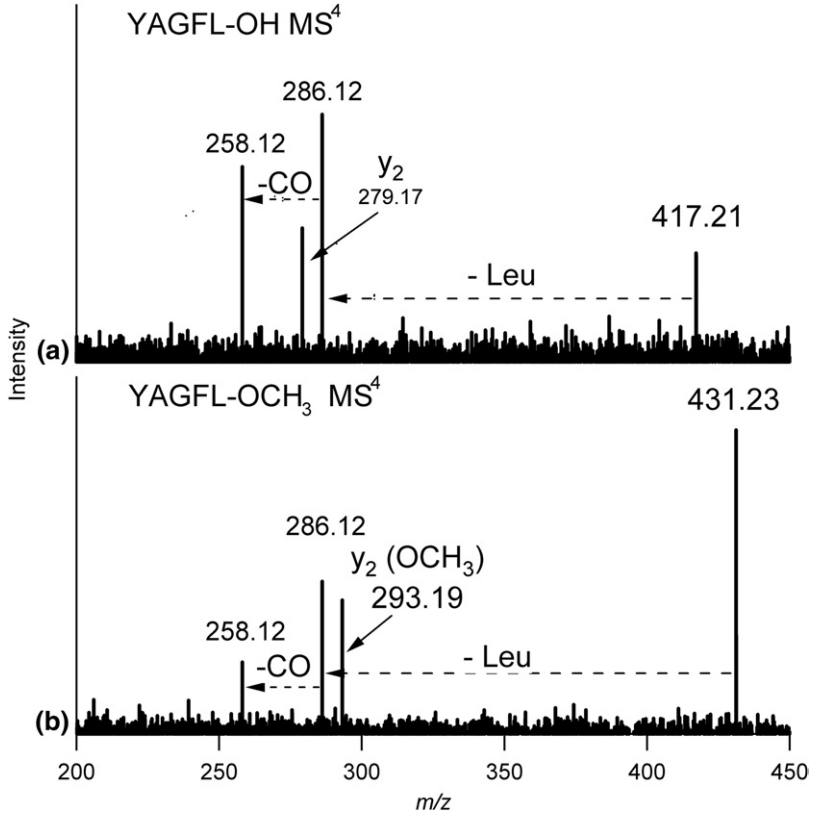

Figure 2. IRMPD MS^4 spectra of fragments at *m/z* 417.21 ($C_{21}H_{29}N_4O_5$) and 431.23 ($C_{22}H_{31}N_4O_5$) generated by in source fragmentation of MH+ (70 eV) and QCID (10 eV) of *m/z* 552.28 and *m/z* 566.30 from protonated (**a**)YAGFL-OH and (**b**)YAGFL-OCH_3, respectively.

fragmentation pathway. The presence of this fragment suggests that an additional ion structure is present at *m/z* 552.28. As previously proposed by both Gaskell and O'Hair for a variety of model peptides, likely the non-C-terminal water loss structure is a valid alternative [11, 33, 34]. The absence of the *m/z* 417.21 fragment from the YAGFL-NH_2 b_5 MS^3 fragment ion spectrum further supports that the $[MH - NH_3]^+$ from YAGFL-NH_2 (*m/z* 552.28) has a b_5 structure, whereas the MS^3 fragmentation spectrum of *m/z* 552.28 from the YAGFL-OH precursor is a mixture of the b_5 and non-C-terminal water loss structures.

IRMPD fragmentation of the *m/z* 417.21 ion is shown in Figure 2 along with an MS^4 spectrum of the *m/z* 431.23 fragment derived from the water loss ion (*m/z* 566.31) from the YAGFL-OCH_3 precursor (the methyl ester analogue of the same non-C-terminal water loss fragment). To obtain these MS^4 spectra, in-source fragmentation with a skimmer voltage of 70 eV was used. The fragment at *m/z* 552.28 (566.30 for the methyl ester) is then fragmented via QCID to yield the fragment at *m/z* 417.21 (431.22 for YAGFL-OCH_3), which is then further fragmented via IRMPD in the ICR cell. Both spectra contain y_2 ions at *m/z* 279.17 and 293.19, respectively, indicating that the C-terminus is still intact and that water must be lost from a position closer to the N-terminus than the second carbonyl from the C-terminus. Additional fragments represent the loss of leucine and a CO, additionally supporting that the *m/z* 417.21 fragment arises from a non-C-terminal $[MH - H_2O]^+$ ion structure; the C-terminus again must be intact for loss of the entire C-terminal residue. The dominance of the fragment at *m/z* 417.21 for the water loss ion is important to recognize because of the potential for error it generates for spectral prediction based on kinetic modeling [9, 35]. Accounting for multiple structures would

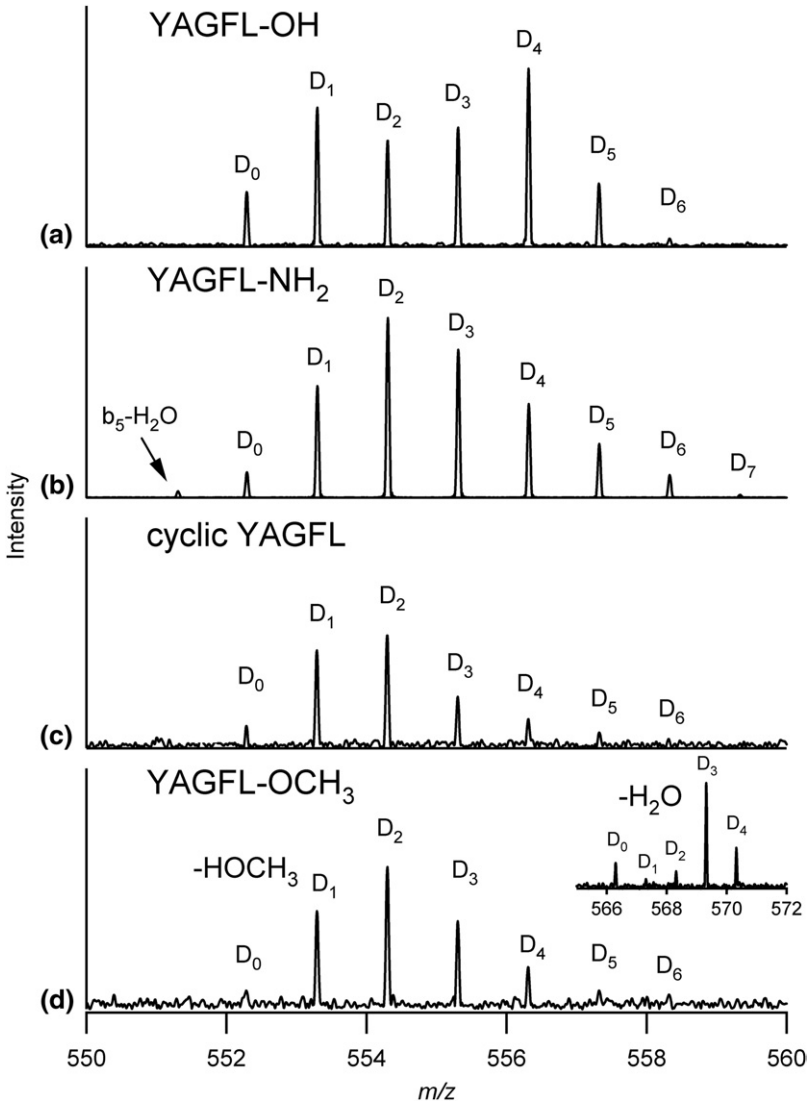

Figure 3. QCID-HDX for the ions at *m/z* 552.28 ($C_{29}H_{38}N_5O_6$) generated from (**a**) YAGFL-OH (-H_2O), (**b**) YAGFL-NH_2 (-NH_3), (**c**) MH^+ of cyclic YAGFL, and (**d**) YAGFL-OCH_3 (-$HOCH_3$) species. In (**d**), the $[MH - H_2O]^+$ ion is also shown in the range of *m/z* 565-573 as an inset.

allow for the kinetics of the multiple fragmentation pathways to be modeled accurately. Additionally, the water loss fragment at *m/z* 417.21 is also present in the MS/MS spectrum of the protonated peptide (see, e.g., Figure S1, which can be found in the electronic version of this article). Formation of this fragment likely occurs by sequential fragmentation of the parent into the fragment at *m/z* 552.28, which could then further fragment to generate typical fragments from both the non-C-terminal water loss and b_5 ion structures. The presence of non-standard fragment ions in MS/MS spectra could interfere with the ability of protein identification algorithms to successfully identify the corresponding peptide sequences.

QCID-HDX

To investigate the possibility of and propensity for separation of the b_5 ion structure from the water loss ion structure for YAGFL-OH, QCID-HDX was performed. QCID-HDX was also performed on YAGFL-OCH_3, YAGFL-NH_2, and cyclic YAGFL for comparison. For this purpose, protonated peptides were first selected by the quadrupole region of the instrument and fragmented in the hexapole collision cell (QCID). Following fragmentation, all ions, including precursor ions and all fragments generated, were introduced into the ICR cell where they were exposed to 50 ms pulses of deuterated methanol (CD_3OD) with a 1s pulse delay between the pulses. Different numbers of pulses were used to determine the relative HDX kinetics for the precursor and all fragment ions (results not shown). It should be noted that while the study of interest is focusing on the ion at *m/z* 552.28, all of the ions were simultaneously exposed to the HDX reagent and underwent different extents of HDX. The QCID-HDX spectrum for YAGFL-OH over the entire mass range can be found in the Supplementary Information (Figure S1). The HDX of the isobaric b_5 and water loss ions for YAGFL-OH and the b_5 ions for YAGFL-NH_2, YAGFL-OCH_3, and the MH^+ of cyclic YAGFL are shown in Figure 3. The water loss from both YAGFL-OH and YAGFL-OCH_3 have HDX patterns reflecting bimodal distributions, whereas YAGFL-NH_2 (-NH_3) shows only a single broad exchange distribution, representative of only b_5 structure(s) with no overlapping water loss ion. The presence of multiple HDX distributions is indicative of differences in structure or protonation sites. Again, the cyclic YAGFL HDX

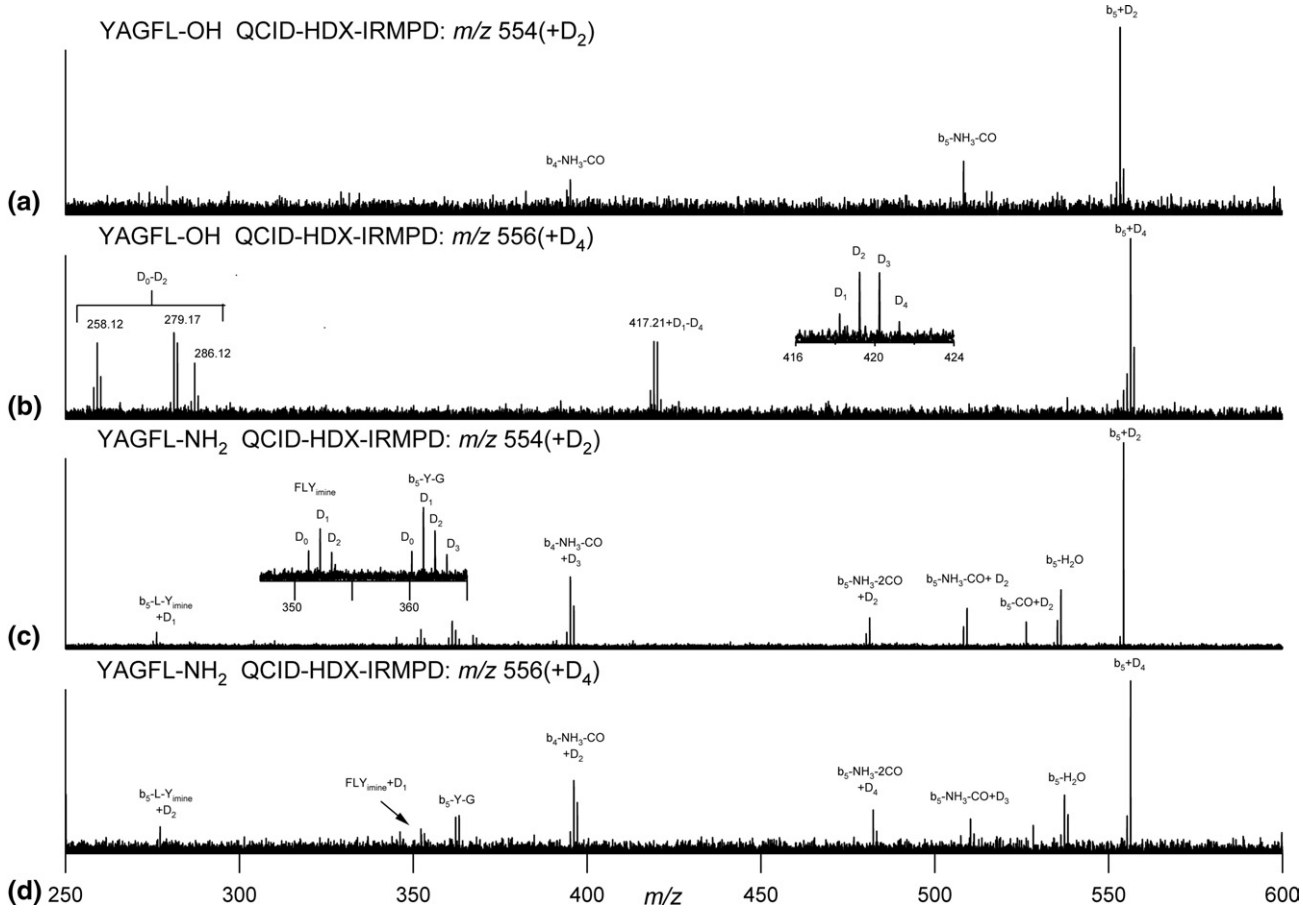

Figure 4. QCID-HDX-IRMPD spectra for the ion at *m/z* 552.28 ($C_{29}H_{38}N_5O_6$) generated from protonated YAGFL-OH with different degrees of HDX. (**a**) D_2, *m/z* 554.3, indicative of b_5 ion structure; (**b**) D_4, *m/z* 556.3, indicative of non-C-terminal $[MH - H_2O]^+$ ion structure. The analogous spectra from YAGFL-NH_2 are shown in (**c**) and (**d**).

at *m/z* 552.28 reflects one of the two proposed b_5 ion structures for YAGFL-NH_2. While the combined exchange population for the b5 ion from YAGFL-NH_2 reflects only a single distribution, the additional exchange beyond that seen for cyclic YAGFL can likely be explained by the contribution of the oxazolone-terminating b_5 ion structure present along with the macrocyclic structure. The bimodal distribution of *m/z* 552.28 from YAGFL-OH is consistent with the overlapping b_5 and $[MH - H_2O]^+$ ion populations that are present. It should also be noted that while multiple distributions reflect additional populations in relation to a single HDX distribution, a single distribution may contain multiple structures that are too similar in exchange behavior and structure to be discerned using this technique. However, the distinct shift from single to multiple exchange distributions clearly reflects the presence of at least one additional structure for *m/z* 552.28 from YAGFL-OH.

To confirm that the faster exchanging HDX population for YAGFL-OH is a result of non-C-terminal water loss, the YAGFL methyl ester (YAGFL-OCH_3) was prepared and analyzed via QCID-HDX. The QCID-HDX of both the b_5 ion formed by CH_3OH loss (*m/z* 552.28) and the non-C-terminal water loss ion (*m/z* 566.30) are also shown in Figure 3. While the HDX for the b_5 ion features a single distribution, at least two populations are shown in the exchange distribution of the water loss ion (see inset in Figure 3d).The multiple populations for the water loss ion distribution may reflect multiple potential water loss structures, as predicted by Gaskell and O'Hair [11, 13].

QCID-HDX-IRMPD

For further structural confirmation that the YAGFL-OH bimodal HDX distribution results from separation of the b_5 and $[MH - H_2O]^+$ ion, ions reflecting different numbers of hydrogen-deuterium exchange (e.g., D_0, D_2, D_4, etc.) were monoisotopically selected and fragmented by IRMPD. The combined QCID-HDX-IRMPD fragmentation spectra for the D_2 and D_4 ions are shown in Figure 4a and 4b; the combined QCID-IRMPD fragmentation spectrum of YAGFL-OH (no exchange) is available for comparison in Figure 1a. The D_2 ion population (*m/z* 554.30) represents predominantly the slower exchanging b_5 population, whereas the D_4 (*m/z* 556.31) represents the faster exchanging $[MH - H_2O]^+$ ion population. The D_4 fragmentation spectrum features predominant fragments at *m/z* 419.23, 420.23, and 421.24, corresponding to the *m/z* 417.21 fragment with two to four deuteriums incorporated, again indicative of the N-terminal loss of tyrosine imine. This ion appears in the composite MS^3 spectrum of *m/z* 552.28 from YAGFL-OH (see Figure 1a). This fragment is absent from the D_2 ion fragmentation spectrum, Figure 4a, which instead features dominant fragment peaks at *m/z* 394.18 and 507.27, which correspond to the b_4-NH_3-CO and b_5-NH_3-CO (a_5-NH_3) fragments, respectively. These fragments are also seen in the b_5 fragmentation spectra from YAGFL-NH_2, YAGFL-OCH_3, and cyclic YAGFL. When no HDX is performed, the structures are not separated, therefore fragments from both the b_5 and non-C-terminal water loss structures are present in the combined QCID-IRMPD (Figure 1a). The separation by HDX and subsequent fragmentation of

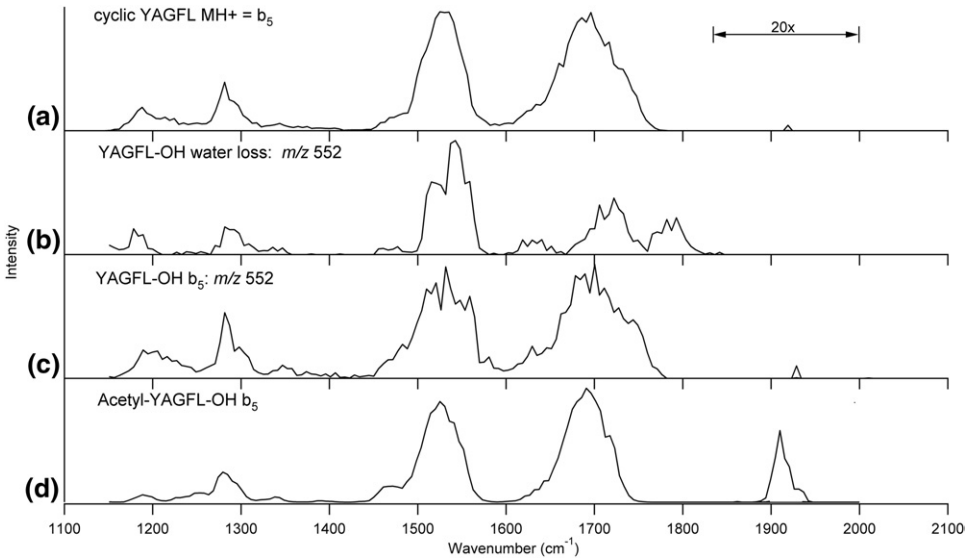

Figure 5. IRMPD spectra of *m/z* 552.28 from (**a**) cyclic YAGFL, (**b**) YAGFL-OH, generated by using the *m/z* 417.21 fragment ion intensity, reflecting the non-C-terminal water loss structure, (**c**) YAGFL-OH, generated by summing all the fragments from the b_5 ion structure. (**d**) IRMPD spectrum of *m/z* 594.30 from acetylated YAGFL, corresponding to the acetylated b_5 ion. All spectra are magnified 20-fold in the oxazolone stretch region.

the b_5 and $[MH - H_2O]^+$ ion structures for YAGFL-OH clearly demonstrates the ability to both separate and characterize gas-phase ions using QCID-HDX-IRMPD.

To differentiate between the different structures for *m/z* 552.28 for YAGFL-OH as opposed to only the multi-component b_5 structure for YAGFL-NH_2, the corresponding QCID-HDX-IRMPD fragmentation spectra of the D_2 and D_4 ion populations are shown in Figure 4c and d, and the QCID-IRMPD spectrum of *m/z* 552.28 from YAGFL-NH_2 is included in Figure 1b. Unlike YAGFL-OH, the fragmentation spectra of D_2 and D_4 from YAGFL-NH_2 feature the same fragmentation patterns, supporting that both of these ions in the exchange population are from the same structure. It is interesting to note that Figure 4a is not identical to Figure 4 c and d, suggesting that the b_5 ions formed by H_2O loss from YAGFL-OH versus NH_3 loss from YAGFL-NH_2 are not identical, perhaps because they consist of different proportions of macrocycle versus oxazolone and/or because they have different internal energy content after loss of the different small neutral molecules.

IRMPD Spectroscopy of YAGFL-OH, cYAGFL, and Acetylated YAGFL

For additional evidence for different structural isomers of the *m/z* 552.28 from different YAGFL derivatives, IRMPD spectroscopy was performed on the *m/z* 552.28 ion corresponding to the MH^+ for cyclic YAGFL, the b_5 and $[MH - H_2O]^+$ for YAGFL-OH, and the b_5 for acetylated YAGFL-OH (*m/z* 594.3 for Acetyl-YAGFL). The corresponding spectra are shown in Figure 5 with quite similar spectra for cyclic YAGFL (Figure 5a) and the b_5 ion (Figure 5c). The IRMPD spectra reflect the relative fragment to parent ion intensity at each wavenumber in the spectrum. Figure 5b shows the IRMPD spectrum of *m/z* 552.28 resulting from the generation of the fragment at *m/z* 417.21, which arises only from the non-C-terminal water loss isomer of *m/z* 552.28. The additional stretch at ~1785 cm^{-1} corresponds to a *m/z* 552.28 structural isomer that is different from the cyclic YAGFL and YAGFL b_5 isomers of *m/z* 552.28. All other reasonably abundant fragment ions generated during IRMPD fragmentation at CLIO can be attributed to fragmentation of the b_5 ion structure and were used to construct the b_5 ion IRMPD spectrum shown in Figure 5c. As expected, acetylation of YAGFL-OH blocks the N-terminus, which prevents the b_5 oxazolone from isomerizing into the cyclic b_5 structure; this explains the presence of the stretch near 1920 cm^{-1}, a region in the spectrum indicative of the oxazolone C=O stretch.

QCID-HDX of Sequence Analogues

To explore the influence of amino acid sequence on the relative percentage of ions present in the b_5 structure versus the water loss ion structure, a series of YAGFL analogues were subjected to QCID-HDX. Although the peptide sequences were varied, the overall amino acid composition of all peptides remained constant. Relative differences in the proportion of b_5 versus water-loss ions can therefore be attributed solely to the location of specific residues. The corresponding QCID-HDX spectra for the fragment ions at *m/z* 552.28 for the sequence analogues AGFLY, GFLYA, FLYAG, LYAGF, and LFGAY are shown in Figure 6. While an exhaustive

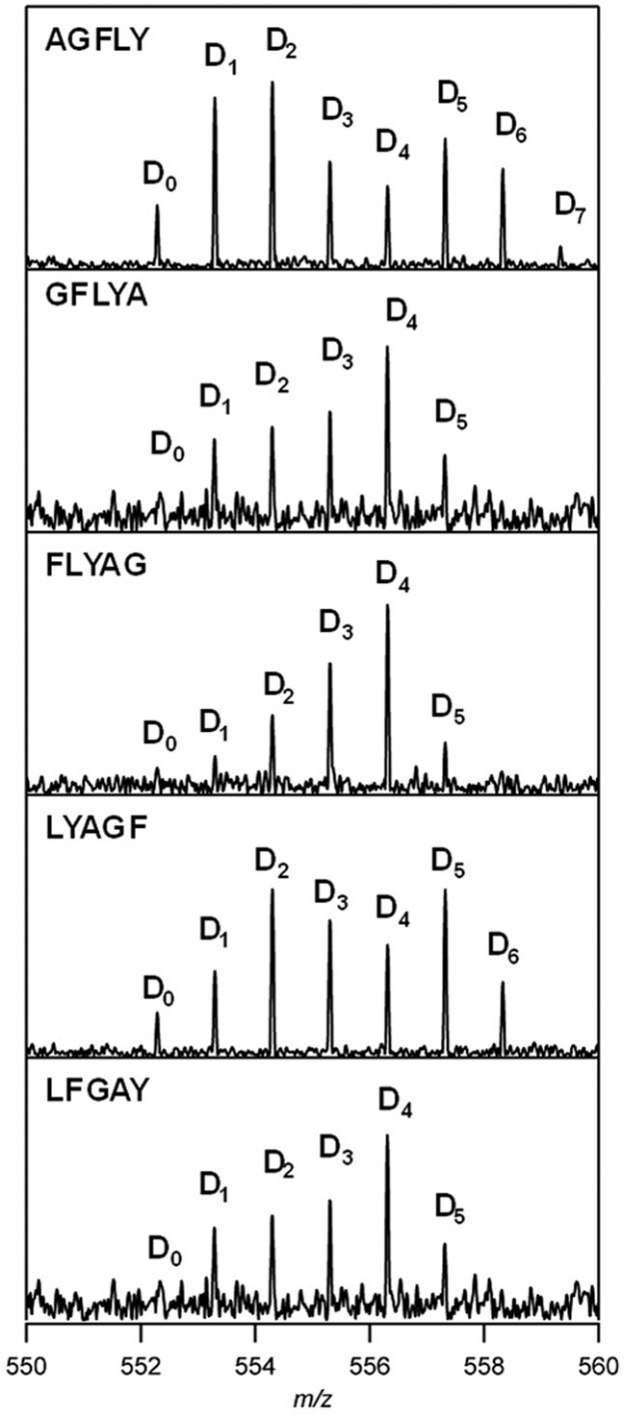

Figure 6. QCID-HDX spectra of the ions at *m/z* 552.28 ($C_{29}H_{38}N_5O_6$) from a variety of YAGFL sequence analogs.

study of all possible sequence locations would be necessary to make a general statement regarding the parameters that affect the relative percentages of b_5 (C-terminal) versus non-C-terminal water loss, these data introduce the idea that the location of a specific residue, without a compositional change, affects the product ion branching ratio for the two types of water loss.

Conclusions

The ability of QCID-HDX-IRMPD to separate isomeric fragment ions from protonated YAGFL-OH and its analogues and to obtain relevant information about their structure has been demonstrated here. The b_5 and $[MH - H_2O]^+$ isomers with a chemical composition of $C_{29}H_{38}N_5O_6$ are likely formed from precursor ions initially protonated at different locations and were separated by gas-phase HDX. The combined QCID-HDX-IRMPD spectra of ions from each HDX population (corresponding to different isomers) revealed different MS^3 fragmentation spectra, characteristic of each isomeric structure. When combined, these spectra form the composite IRMPD MS^3 spectrum of the $C_{29}H_{38}N_5O_6$ fragment. Separation of these isomeric structures is supported by the YAGFL-OCH_3 system, where the b_5 and water loss ions do not overlap. This method demonstrates a relatively simple alternative technique to obtain structural information and to distinguish ion populations. This approach is complementary to other widely used structural characterization techniques, such as ion mobility and variable wavelength IRMPD spectroscopy, and combines the separation and structural characterization into one gas-phase experiment as well as one instrument. Additionally, QCID-HDX-IRMPD could be used as a pre-screening tool before variable wavelength action IRMPD spectroscopy to discern if multiple ion structures are predicted for an action spectrum, enabling sometimes complex action IRMPD spectra to be interpreted more readily. This technique might also be used following an ion mobility separation of ions based on their collisional cross-sections, allowing for additional structural information to be obtained for ions formed by MS/MS.

Acknowledgments

The authors thank Asiri Galhena for preliminary experiments, the University of Arizona Mass Spectrometry Facility, and NIH grant GM R01 51387 awarded to VHW. The aid and expertise of the CLIO staff (P. Maitre, J. Lemaire, B. Rieul, R. Singha, V. Steinmetz, and C. Six) as well as funding from the EPITOPES project for beam time is grateful acknowledged. Gary Kruppa of Bruker Daltonics is also gratefully acknowledged for his assistance with pulse sequence implementation.

Appendix A
Supplementary Material

Supplementary material associated with this article may be found in the online version at doi:10.1016/j.jasms.2010.03.036.

References

1. Hunt, D. F.; Yates, J. R.; Shabanowitz, J.; Winston, S.; Hauer, C. R. Protein Sequencing by Tandem Mass Spectrometry. *Proc. Natl. Acad. Sci. U. S. A.* **1986,** *83,* 6233–6237.
2. Aebersold, R.; Mann, M. Mass Spectrometry-Based Proteomics. *Nature* **2003,** *422,* 198–207.
3. Eng, J. K.; McCormack, A. L.; Yates, J. R. An Approach to Correlate Tandem Mass Spectral Data of Peptides with Amino Acid Sequences in a Protein Database. *J. Am. Soc. Mass Spectrom.* **1994,** *5,* 976–989.
4. Perkins, D. N.; Pappin, D. J.; Creasy, D. M.; Cottrell, J. S. Probability-Based Protein Identification by Searching Sequence Databases Using Mass Spectrometry data. *Electrophoresis* **1999,** *20,* 3551–3567.
5. Dongre, A. R.; Jones, J. L.; Somogyi, A.; Wysocki, V. Influence of Peptide Composition, Gas-Phase Basicity, and Chemical Modification on Fragmentation Efficiency: Evidence for the Mobile Proton Model. *J. Am. Chem. Soc.* **1996,** *118,* 8365–8374.
6. Paizs, B.; Suhai, S. Fragmentation Pathways of Protonated Peptides. *Mass Spectrom. Rev.* **2005,** *24,* 508–548.
7. Elias, J. E.; Gibbons, F. D.; King, O. D.; Roth, F. P.; Gygi, S. P. Intensity-Based Protein Identification by Machine Learning from a Library of Tandem Mass Spectra. *Nat. Biotechnol.* **2004,** *22,* 214–219.
8. Nesvizhskii, A. E.; Vitek, O.; Aebersold, R. Analysis and Validation of Proteomic Data Generated by Tandem Mass Spectrometry. *Nat. Methods* **2007,** *4,* 787–797.
9. Resing, K. A.; Meyer-Arendt, K.; Mendoza, A. M.; Aveline-Wolf, L. D.; Jonscher, K. R.; Pierce, K. G.; Old, W. M.; Cheung, H. T.; Russell, S.; Wattawa, J. L.; Goehle, G. R.; Knight, R. D.; Ahn, N. G. Improving Reproducibility and Sensitivity in Identifying Human Proteins by Shotgun Proteomics. *Anal. Chem.* **2004,** *76,* 3556–3568.
10. Tabb, D. L.; Smith, L. L.; Breci, L. A.; Wysocki, V. H.; Lin, D.; Yates, J. R. Statistical Characterization of Ion Trap Tandem Mass Spectra from Doubly Charged Tryptic Peptides. *Anal. Chem.* **2003,** *75,* 1155–1163.
11. Ballard, K. D.; Gaskell, S. J. Dehydration of Peptide [M + H]+ Ions in the Gas Phase. *J. Am. Soc. Mass Spectrom.* **1993,** *4,* 477–481.
12. Reid, G. E.; Simpson, R. J.; O'Hair, R. A. J. A Mass Spectrometric and Ab Initio Study of the Pathways for Dehydration of Simple Glycine and Cysteine-Containing [M + H]+ ions. *J. Am. Soc. Mass Spectrom.* **1998,** *9,* 945–956.
13. Reid, G. E.; Simpson, R. J.; O'Hair, R. A. J. Probing the Fragmentation Reactions of Protonated Glycine Oligomers via Multistage Mass Spectrometry and Gas Phase Ion Molecule Hydrogen/Deuterium Exchange. *Int. J. Mass Spectrom.* **1999,** *190/191,* 209–230.
14. Campbell, S.; Rodgers, M. T.; Marzluff, E. M.; Beauchamp, J. L. Structural and Energetic Constraints on Gas Phase Hydrogen/Deuterium Exchange Reactions of Protonated Peptides with D2O, CD3OD, CD3CO2D, and ND3. *J. Am. Chem. Soc.* **1994,** *116,* 9765–9766.
15. Freitas, M. A.; Marshall, A. G. Rate and Extent of Gas-Phase Hydrogen/Deuterium Exchange of Bradykinins: Evidence for Peptide Zwitterions in the Gas Phase. *Int. J. Mass Spectrom.* **1999,** *182/183,* 221–231.
16. Herrmann, K.; Kuppanan, K.; Wysocki, V. Fragmentation of Doubly-Protonated Peptide Ion Populations Labeled by H/D Exchange with CD3OD. *Int. J. Mass Spectrom.* **2006,** *249,* 93–105.
17. Mazurek, U.; McFarland, M. A.; Marshall, A. G.; Lifshitz, C. Isolation of Isomers Based on Hydrogen/Deuterium Exchange in the Gas Phase. *Eur. J. Mass Spectrom.* **2004,** *10,* 755–758.
18. Chen, X.; Yu, L.; Steill, J.; Oomens, J.; Polfer, N. C. Effect of Peptide Fragment Size on the Propensity of Cyclization in Collision-Induced Dissociation: Oligoglycine b2-b8. *J. Am. Chem. Soc.* **2009,** 131(51), 18977–18982.
19. Bythell, B. J.; Somogyi, A.; Paizs, B. What is the Structure of b2 Ions generated from Doubly Protonated Tryptic Peptides? *J. Am. Soc. Mass Spectrom.* **2009,** *20,* 618–624.
20. Somogyi, A. Probing Peptide Fragment Ion Structures by Combining Sustained Off-Resonance Collision-Induced Dissociation and Gas-Phase H/D Exchange (SORI-HDX) in Fourier Transform Ion-Cyclotron Resonance (FT-ICR) Instruments. *J. Am. Soc. Mass Spectrom.* **2008,** *19,* 1771–1775.
21. Riba-Garcia, I.; Giles, K.; Bateman, R. H.; Gaskell, S. J. Evidence for Structural Variants of a- and b-Type Peptide Fragment Ions Using Combined Ion Mobility/Mass Spectrometry. *J. Am. Soc. Mass Spectrom.* **2008,** *19,* 609–613.
22. Polfer, N. C.; Bohrer, B. C.; Plasencia, M. D.; Paizs, B.; Clemmer, D. E. On the Dynamics of Fragment Isomerization in Collision-Induced Dissociation of Peptides. *J. Phys. Chem. A* **2008,** *112,* 1286–1293.
23. Oomens, J.; Young, S.; Molesworth, S.; van Stipdonk, M. Spectroscopic Evidence for an Oxazolone Structure of the b2 Fragment Ion

from Protonated Tri-Alanine. *J. Am. Soc. Mass Spectrom.* **2009,** *2009,* 334–339.
24. Polfer, N. C.; Oomens, J.; Suhai, S.; Paizs, B. Spectroscopic and Theoretical Evidence for Oxazolone Ring Formation in Collision-Induced Dissociation of Peptides. *J. Am. Chem. Soc.* **2005,** *127,* 17154–17155.
25. Yoon, S. H.; Chamot-Rooke, J.; Perkins, B. R.; Hilderbrand, A. E.; Poutsma, J. C.; Wysocki, V. H. IRMPD. Spectroscopy Shows That AGG Forms an Oxazolone b2+ Ion. *J. Am. Chem. Soc.* **2008,** *130,* 17644–17645.
26. Perkins, B. R.; Chamot-Rooke, J.; Yoon, S. H.; Gucinski, A. C.; Somogyi, A.; Wysocki, V. Evidence for Diketopiperazine and Oxazolone Structures for HA b2+ Ion. *J. Am. Chem. Soc.* **2009,** *131,* 17528–17529.
27. Eyler, J. R. Infrared Multiple Photon Dissociation Spectroscopy of Ions in Penning Traps. *Mass Spectrom. Rev.* **2009,** *28,* 468–494.
28. Polfer, N. C.; Oomens, J. Vibrational Spectroscopy of Bare and Solvated Ionic Complexes of Biological Relevance. *Mass Spectrom. Rev.* **2009,** *28,* 468–494.
29. Polfer, N. C.; Oomens, J.; Suhai, S.; Paizs, B. Infrared Spectroscopy and Theoretical Studies on Gas-Phase Protonated Leu-enkephalin and Its Fragments: Direct Experimental Evidence for the Mobile Proton. *J. Am. Chem. Soc.* **2007,** *129*(18), 5887–5897.
30. Atherton, E.; Sheppard, R. C. Solid-Phase Peptide Synthesis: A Practical Approach; Oxford University Press: Oxford, 1989.
31. Bleiholder, C.; Osburn, S.; Williams, T. D.; Suhai, S.; Van Stipdonk, M.; Harrison, A. G.; Paizs, B. Sequence-Scrambling Fragmentation Pathways of Protonated Peptides. *J. Am. Chem. Soc.* **2008,** *130,* 17774–17789.
32. Harrison, A. G.; Young, A. B.; Bleiholder, C.; Suhai, S.; Paizs, B. Scrambling of Sequence Information in Collision-Induced Dissociation of Peptides. *J. Am. Chem. Soc.* **2006,** *75,* 1524–1535.
33. Reid, G. E.; Simpson, R. J.; O'Hair, R. A. J. A Mass Spectrometric and Ab Initio Study of the Pathways for Dehydration of Simple Glycine and Cysteine-Containing Peptide $[M + H]^+$ ions. *J. Am. Soc. Mass Spectrom.* **1998,** *9,* 945–956.
34. Bleiholder, C.; Osburn, S.; Williams, T. D.; Suhai, S.; Van Stipdonk, M.; Harrison, A. G.; Paizs, B. Sequence-Scrambling Fragmentation Pathways Protonated Peptides. *J. Am. Chem. Soc.* **2008,** *130,* 17774–17789.
35. Zhang, Z. Prediction of Low-Energy Collision Induced Dissociation Spectra of Peptides. *Anal. Chem.* **2004,** *76,* 3908–3922.